Optical and Electrical Properties of Organic Semiconductor Thin Films for Optoelectronic Devices

Zhong Zhiyou[1,2], *Zhu Ya*[1], *Chen Shoubu*[1], *Lu Zhou*[1]

(1 College of Electronics Information Engineering, South-Central University for Nationalities, Wuhan 430074, China;
2 Hubei Key Laboratory of Intelligent Wireless Communications, South-Central University for Nationalities, Wuhan 430074, China)

Abstract Organic semiconductor thin films of tris(8-hydroxy-quinoline) aluminum (AlQ), aluminum (III) bis(2-methyl-8-quninolinato)-4-phenylphenolate (BAlQ), and α-naphthylphenylbiphenyl amine (NPB) were deposited by vacuum sublimation. The transmission, abosorption and the optical properties of the thin films were investigated. In addition, the thin film devices of sandwich structure were fabricated and the current-voltage characteristics were studied. The results showed that the organic thin films were highly transparent. AlQ and BAlQ demonstrated almost the same direct energy bandgap (4.46 eV), which was larger than that of NPB (3.11 eV). The internal free carrier density of AlQ, BAlQ and NPB were of the same order of magnitude (10^{22} m^{-3}), whereas NPB exhibited the highest zero-field mobility (1.75×10^{-8} $cm^2 \cdot V^{-1} \cdot s^{-1}$) and electrical conductivity (1.45×10^{-10} $S \cdot cm^{-1}$).

Keywords sorganic semiconductor, thin film, optical and electrical properties

中图分类号 TN383 **文献标识码** A **文章编号** 1672-4321(2018)04-0067-06

光电器件中有机半导体薄膜的光学和电学性质研究

钟志有[1,2], 朱 雅[1], 陈首部[1], 陆 轴[1]

(1 中南民族大学 电子信息工程学院,武汉 430074; 2 中南民族大学 智能无线通信湖北省重点实验室, 武汉 430074)

摘 要 采用真空热蒸发制备了 AlQ, BAlQ 和 NPB 有机半导体薄膜样品,探讨了薄膜的透射、吸收和光学性质.制备了有机薄膜样品的夹心结构器件,研究了其电流-电压特性.结果表明: 有机薄膜的透明性能良好, AlQ 和 BAlQ 具有几乎相同的直接光学能隙(4.46 eV),大于 NPB 的能隙值(3.11 eV). AlQ, BAlQ 和 NPB 内部自由载流子浓度具有相同的数量级(10^{22} m^{-3}),但 NPB 具有最高的零电场迁移率(1.75×10^{-8} $cm^2 \cdot V^{-1} \cdot s^{-1}$)和电导率($1.45\times10^{-10}$ $S \cdot cm^{-1}$).

关键词 有机半导体; 薄膜; 光电性质

In recent years, a considerable amount of research has been carried out on the organic semiconductors which is becoming an attractive alternative to inorganic semiconductors for applications in optoelectronic devices, for instance, photovoltaic solar cells[1-3], electroluminescent diodes[4-6], electrochromic devices[7,8], light-emitting electrochemical cells[9-11] and organic semiconductor lasers[12,13]. In parallel with these activities, many researchers have made much progress in the understanding of the underlying physics that controls the properties of these devices. In comparison with inorganic semiconductors, however, much less is known about the optical and electrical properties of the organic semiconductors which are crucial to the structure design and performance improvement of the optoelectronic devices. In this study, the thin films of tris(8-hydroxy-quinoline) aluminum (AlQ), aluminum (III) bis(2-methyl-8-quninolinato)-4-phenylphenolate (BAlQ), and α-naphthylphenylbiphenyl amine (NPB) were prepared

收稿日期 2017-12-06

作者简介 钟志有(1965-),男,教授,博士,研究方向: 能源光电子、信息功能材料与器件, E-mail: zhongzhiyou@163.com

基金项目 湖北省自然科学基金资助项目(2011CDB418); 中央高校基本科研业务专项资金资助项目(CZP17002)

by the vacuum sublimation technique. The optical properties of the thin films were investigated by optical transmittance, absorbance spectra and energy bandgap. Furthermore, single-layer thin film devices were fabricated, and the electrical properties of the materials were studied through the measurements of current-voltage characteristics, electrical conductivity and charge carrier mobility.

Organic semiconductor materials of AlQ, BAlQ and NPB were purchased from Sigma-Aldrich Chemical Company and used as-received. The molecular structures of the materials are shown in Fig. 1. Commercially quartz glass was used as substrates to prepare organic semiconductor thin films and single-layer devices in this experiment.

1 Experimental procedure

1.1 Materials

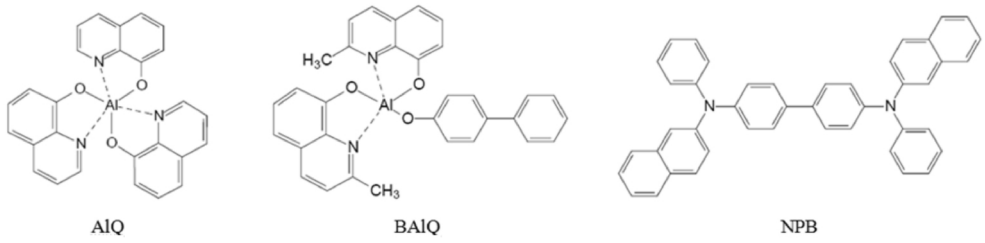

Fig.1 Molecular structures of organic semiconductor materials of AlQ, BAlQ and NPB

图 1 有机半导体材料 AlQ, BAlQ 和 NPB 的分子结构图

1.2 Substrate cleaning

Substrate cleaning plays an important role in the deposition of thin films. The quartz glass was cut into 3 cm×3 cm plates in this experiment. Prior to their use, it was routinely cleaned by rubbing first with detergent and then with the mixture of aether and alcohol (the volume ratio of aether to alcohol is 1 : 1), followed by rinsing in deionized water, and finally dried in a flow of nitrogen.

1.3 Thin film deposition

Using the previously cleaned quartz glass as substrates, the organic semiconductor thin films of AlQ, BAlQ and NPB were prepared by vacuum evaporation, respectively. The thermal evaporation process was performed by a suitable quartz crucible with a multifunctional deposition system of OLED-V at a base pressure of about 2×10^{-5} Pa. During the deposition process, the substrate was kept at about 310 K. The glass substrate was also rotated during the deposition process by means of a rotary working holder at a speed of 20 r/min so as to obtain a uniform thickness of thin films. The deposition rate was controlled to be about 0.1 nm·s^{-1}, and it was continuously measured by a quartz oscillating thickness monitor. The thickness of AlQ, BAlQ and NPB thin films are all approximately 100 nm.

1.4 Devices fabrication

In order to study the electrical properties of organic semiconductor thin films, the single-layer devices with the structure of glass/Al (200 nm)/organic layer (100 nm)/Al (200 nm) were fabricated by the vacuum sublimation technique. The effective area was defined by a shadow mask with 0.6 cm×0.6 cm patterns. All layers were continuously deposited under the base pressure of about 2×10^{-5} Pa without breaking the vacuum. The deposition rates of aluminium and organic materials are about 0.3 and 0.1 nm·s^{-1}, respectively.

1.5 Characterization methods

The transmittance and absorbance of the thin films were recorded by a double beam spectrophotometer of Perkin Elmer Lambda 900 UV/VIS/NIR, respectively. The current-voltage (J-V) characteristics of the single-layer devices were measured using a Keithley-4200 source measure unit. All measurements were carried out at room temperature (about 300 K) under ambient conditions.

2 Results and discussion

2.1 Optical properties

The optical transmission spectra of all the thin films are depicted in Fig.2. Inspection of Fig.2 shows that these thin films are highly transparent in the spectral range from 460 to 800 nm. The high transparency indicates the small surface roughness and the better homogeneity of the thin films. The transmission of the thin films decreases obviously when the wavelength is reduced to around 460 nm. As can be seen, the fundamental absorption edge is closely related to the used materials. The fundamental absorption edge (λ_0) of thin films AlQ, BAlQ and NPB are located at 270-300, 260-320 and 350-440 nm, respectively. The absorption edge of these materials gives the energy bandgap (E_g), and the relationship between E_g and the position of the normally sharp absorption edge is described as [14]:

$$E_g = \frac{hc}{\lambda_0}, \qquad (1)$$

where h is Planck's constant, c velocity of light, and λ_0 is wavelength of absorption edge. At high absorption levels, the relationship between absorption coefficient (α) and E_g is expressed to calculate energy bandgap of the thin films by the following formula [15]:

$$\alpha h\nu = C(h\nu - E_g)^p, \qquad (2)$$

where C is an energy-independent constant, p is an exponent which can assume values of 1/2, 3/2, 2 and 3 depending on the nature of the electronic transitions responsible for optical absorption. $p = 1/2$ and 3/2 for direct allowed and forbidden transitions, respectively, $p = 2$ and 3 for indirect allowed and forbidden transition, respectively [16].

Fig.3 shows the optical absorbance spectra of all the thin films as a function of wavelength. The absorption coefficient α was calculated using the following equation:

$$\alpha = 2.303\frac{A}{d}, \qquad (3)$$

where A is the measured absorbance and d the thickness of the films. Fig.4 shows the typical curves of $(\alpha h\nu)^2$ versus $h\nu$ for all the thin films at room temperature. The values of E_g were obtained by

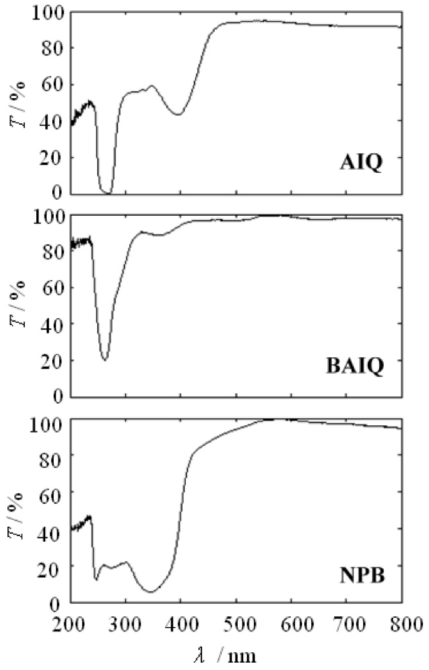

Fig.2　Transmission spectra of the thin films AlQ, BAlQ and NPB

图 2　薄膜 AlQ, BAlQ 和 NPB 的透射谱

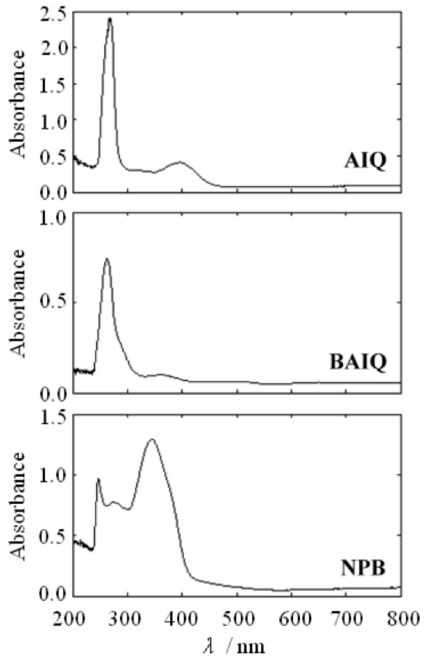

Fig.3　Absorbance of the thin films AlQ, BAlQ and NPB

图 3　薄膜 AlQ, BAlQ 和 NPB 的吸光度

extrapolation of the linear portion of the graph to $(\alpha h\nu)^2 = 0$ [17]. A good straight line is obtained with $p = 1/2$ for all the thin films. The observed values E_g (direct transitions) for the prepared thin films are tabulated in Tab.1. Note that the E_g values of thin films AlQ, BAlQ and NPB are 4.46, 4.47 and 3.11 eV, respectively. Clearly, AlQ and BAlQ share the almost same E_g value, and the E_g values of AlQ and BAlQ are

larger than that of NPB.

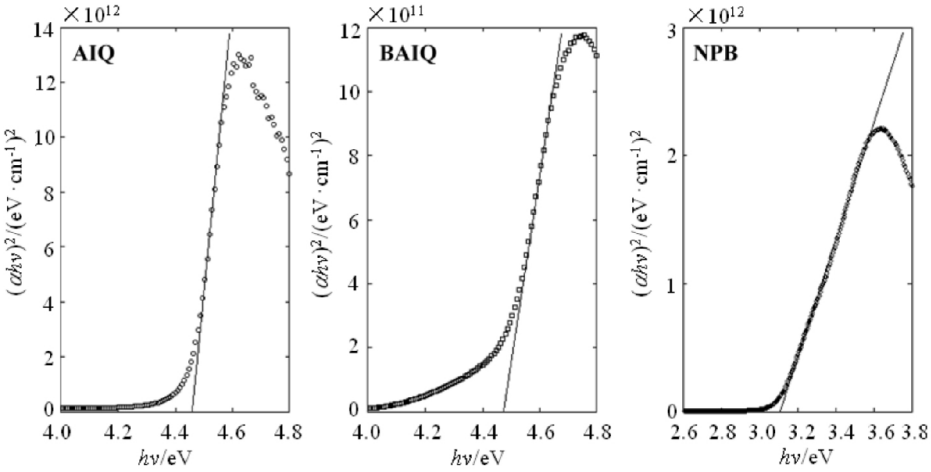

Fig.4 $(\alpha h\nu)^2$-$h\nu$ curves for thin films of AlQ, BAlQ and NPB

图 4 薄膜 AlQ, BAlQ 和 NPB 的$(\alpha h\nu)^2$-$h\nu$ 曲线

Tab.1 Optical and electrical properties for thin films of AlQ, BAlQ and NPB

表 1 薄膜 AlQ, BAlQ 和 NPB 的光电性质

Sample	E_g/eV	V_t/V	μ_0/cm$^2\cdot$V$^{-1}\cdot$s^{-1}	β/cm$^{1/2}\cdot$V$^{-1/2}$	n_0/m^{-3}	σ/S$\cdot$cm^{-1}
AlQ	4.46	3.9	1.63×10^{-11}	2.94×10^{-4}	8.49×10^{22}	1.98×10^{-13}
BAlQ	4.47	4.4	5.58×10^{-9}	5.87×10^{-4}	9.58×10^{22}	7.58×10^{-11}
NPB	3.11	2.8	1.75×10^{-8}	5.65×10^{-4}	6.10×10^{22}	1.45×10^{-10}

2.2 Electrical properties

Fig.5 gives the current-voltage (*J*-*V*) characteristics of all the thin films at room temperature. From the double logarithmic plot, it can be seen that the *J*-*V* curves follow a power law of the form $J \propto V^m$ with different slopes in the lower and higher voltage regions, where m is a power index. At low voltages there is a $m=1$ region corresponding to an ohmic region where the current density J is proportional to the voltage V. At higher voltages, there is a transition to a $m=2$ region, corresponding to the onset of space-charge limited conduction (SCLC). At still higher voltages there is a transition to a region of even higher m value, corresponding to a region where the traps within the material become filled, resulting in a sharp increase in current density J.

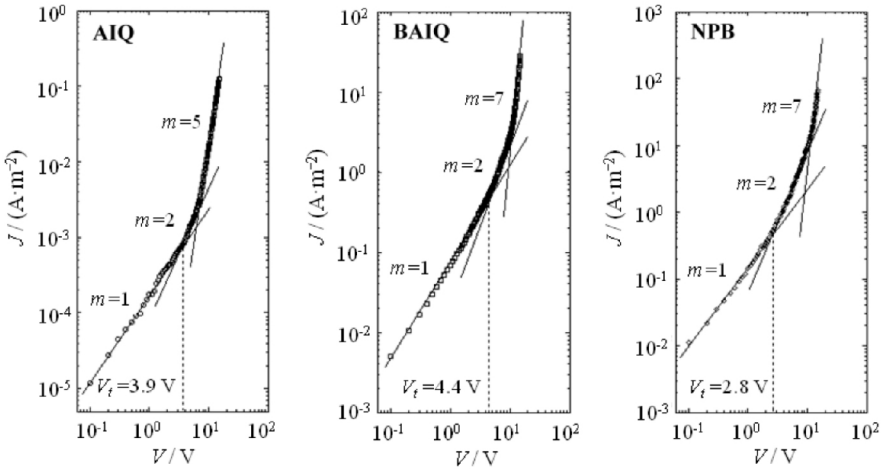

Fig.5 *J*-*V* characteristics curves for thin films of AlQ, BAlQ and NPB

图 5 薄膜 AlQ, BAlQ 和 NPB 的 *J*-*V* 曲线图

In theohmic region of $m=1$, the *J*-*V* characteristics obey the Ohm's law and the current density J can be

expressed as [18,19]:

$$J = \sigma \frac{V}{d}, \quad (4)$$

where σ is the electrical conductivity, and d the film thickness.

In the SCLC region of $m = 2$, the J–V characteristics follow the Mott–Gurney equation [20,21]:

$$J = \frac{9}{8}\varepsilon\mu\frac{V^2}{d^3}, \quad (5)$$

where μ is the carrier mobility, $\varepsilon = \varepsilon_0\varepsilon_r = 3.1\times10^{-11}$ F · m^{-1} is the permittivity of organic layer. According to the Poole–Frenkel law, the relation between μ and E can be represented as [22,23]:

$$\mu = \mu_0\exp(0.89\beta\sqrt{E}), \quad (6)$$

where μ_0 is the zero-field mobility, β the Poole–Frenkel coefficient, and $E = V/d$ is the applied electric field. According to the equations (4) and (5), the J–V characteristics can be described by the following equation:

$$J = \frac{9}{8}\varepsilon\mu_0\frac{E^2}{d}\exp(0.89\beta\sqrt{E}). \quad (7)$$

From Eq.(6), we get:

$$\ln\left(\frac{J}{E^2}\right) = 0.89\beta\sqrt{E} + \ln\left(\frac{9\varepsilon}{8d}\mu_0\right). \quad (8)$$

Equation (8) indicates that $\ln(J/E^2)$ is proportional to $\sqrt{E}$ in the SCLC region. The experimental data for the SCLC region of all the thin films can be fit to a straight line according to Eq.(8), and the values of μ_0 and β were obtained and summarized in Tab.1. Note that for the thin films AlQ, BAlQ and NPB, the values $\mu_0 = 1.63\times10^{-11}$ cm^2 · V^{-1} · s^{-1}, $\beta = 2.94\times10^{-4}$ cm$^{1/2}$ · V$^{-1/2}$, $\mu_0 = 5.58\times10^{-9}$ cm^2 · V^{-1} · s^{-1}, $\beta = 5.87\times10^{-4}$ cm$^{1/2}$ · V$^{-1/2}$ and $\mu_0 = 1.75\times10^{-8}$ cm^2 · V^{-1} · s^{-1}, $\beta = 5.65\times10^{-4}$ cm$^{1/2}$ · V$^{-1/2}$, respectively. Similar values of μ_0 have been reported for conjugated dendrimers, poly (paraphenylene vinylene) and its derivatives by Lupton, Meyer and Conwell et al [24–26]. In our present work, NPB shows the highest μ_0 value, while AlQ processes the lowest μ_0 value. Clearly, the μ_0 value of NPB is about three orders of magnitude greater than that of AlQ at room temperature.

When combining Eq.(4) and (5) with the formula $\sigma = n_0q\mu$, the free carrier density n_0 can be determined by the following relation:

$$n_0 = \frac{9}{8}\frac{\varepsilon V_t}{qd^2}, \quad (9)$$

where q is the magnitude of the electron charge, and V_t is the threshold voltage at which the transition occurs from ohmic conduction to SCLC conduction. Using the values of ε, q, d and V_t (see Fig. 5), the n_0 are calculated out to be about 8.49×10^{22}, 9.58×10^{22} and 6.10×10^{22} m^{-3} for the thin films AlQ, BAlQ and NPB, respectively. As can be seen, the free carrier density n_0 of AlQ, NPB and BAlQ share the same order of magnitude (10^{22} m^{-3}).

In addition, the σ values were evaluated by fitting the experimental data in the ohmic region of Fig. 5 according to Eq. (4), and the results were given in the Tab. 1. Note that the measured values of σ can be observed to decrease in the sequence of NPB, BAlQ, AlQ. NPB exhibits the highest σ value (1.45×10^{-10} S · cm^{-1}), while AlQ gives the lowest σ value (1.98×10^{-13} S · cm^{-1}). The result indicates that electrical conductivity of NPB is superior to those of AlQ and BAlQ.

3 Conclusion

Organic semiconductor thin films AlQ, BAlQ and NPB were prepared, and the optical properties in the UV–visible region of the thin films were investigated at room temperature in terms of the optical transmittance and absorbance spectra measurements. The energy bandgaps of the deposited thin films were calculated. In addition, the single-layer structure devices were fabricated with these organic semiconductor materials, and the electrical properties of the thin films were evaluated through the measurement and analysis of current–voltage characteristics of the devices. Experimental results indicate that the free carrier density of AlQ, NPB and BAlQ share the same order of magnitude, and the zero-field mobility and electrical conductivity of NPB is, respectively, about three orders of magnitude greater than those of AlQ at room temperature.

References

[1] Kato T, Hagiwara N, Suzuki E, et al. Morphology control

for highly efficient organic-inorganic bulk heterojunction solar cell based on Ti-alkoxide [J]. Thin Solid Films, 2016, 600(1): 98-102.

[2] Spanggaard H, Krebs F C. Production of large-area polymer solar cells by industrial silk screen printing, lifetime considerations and lamination with polyethyleneterephthalate [J]. Solar Energy Mater Solar Cells, 2004, 83(2/3): 293-300.

[3] Wang N, Yu J, Zang Y, et al. Effect of buffer layers on the performance of organic photovoltaic cells based on copper phthalocyanine and C60 [J]. Solar Energy Mater Solar Cells, 2010, 94(1): 263-266.

[4] Tang C W, VanSlyke S A. Organic electroluminescent diodes [J]. Appl Phys Lett, 1987, 51(12): 913-915.

[5] Burroughes J H, Bradley D D C, Brown A R, et al. Light-emitting diodes based on conjugated polymers [J]. Nature, 1990, 347(6293): 539-541.

[6] Kim H S, Moon S I, Hwang D E, et al. Novel fabrication method of microlens arrays with High OLED outcoupling efficiency [J]. Opt Laser Technol, 2016, 77(1): 104-110.

[7] Mortimer R J, Dyer A L, Reynolds J R. Electrochromic organic and polymeric materials for display applications [J]. Displays, 2006, 27(1): 2-18.

[8] Yang C H, Chong L W, Huang L M, et al. Novel electrochromic devices based on composite films of poly(2,5-dimethoxyaniline)-waterborne polyurethane [J]. Mater Chem Phys, 2005, 91(2): 154-160.

[9] Alem S, Gao J. The effect of annealing/quenching on the performance of polymer light-emitting electrochemical cells [J]. Org Electron, 2008, 9(3): 347-354.

[10] Edman L, Summers M A, Buratto S K, et al. Polymer light-emitting electrochemical cells: Doping, luminescence, and mobility [J]. Phys Rev B, 2004, 70(11): 2516-2528.

[11] You Z Z, Hua G J. Luminescent and electrical performance of polymer light-emitting electrochemical cells with treated indium-tin-oxide electrodes [J]. Int J Electron, 2010, 97(1): 99-104.

[12] Berggren M, Dodabalapur A, Slusher R E, et al. Organic solid-state lasers with imprinted gratings on plastic substrates [J]. Appl Phys Lett, 1998, 72(4): 410-411.

[13] Zavelani-Rossi M, Lanzani G, Anni M, et al. Organic laser based on thiophene derivatives [J]. Synth Met, 2003, 139(6): 901-903.

[14] Zhong Z, Kang H, Lu Z, et al. Effect of doping on optical properties of zinc oxide semiconductor thin films [J]. J South-Cent Univ Nationlities (Nat Sci Ed), 2017, 36(3): 61-67.

[15] Hua Q, Fu R, Yang W, et al. Effect of sputtering time on the properties of boron-doped ZnO thin films [J]. Mater Rev B, 2013, 27(9): 16-22.

[16] Lu Z, Long L, Zhong Z, et al. Structural characterization and optoelectrical properties of Ti-Ga co-doped ZnO thin films prepared by magnetron sputtering [J]. J Mater Sci: Mater Electron, 2016, 27(3): 2875-2884.

[17] Zhong Z, Kang H, Long H. Preparation and properties of magnesium and yttrium doped zinc oxide thin films [J]. J South-Cent Univ Nationlities (Nat Sci Ed), 2018, 37(1): 66-72.

[18] Zhang Y, Hu Y, Chen J, et al. Charge carrier injection and transport in PVK: Alq_3 blend films [J]. J Phys D: Appl Phys, 2003, 36(16): 2006-2009.

[19] Breeze A J, Schlesinger Z, Carter S A, et al. Charge transport in TiO_2/MEH-PPV polymer photovoltaics [J]. Phys Rev B, 2001, 64(12): 125205-1-2125205-9.

[20] Blom P W M, de Jong M J M, van Munster M G. Electric-field and temperature dependence of the hole mobility in poly.p-phenylene vinylene [J]. Phys Rev B, 1997, 55(2): R656-R659.

[21] Besbes S, Ltaief A, Reybier K, et al. Injection modifications by ITO functionalization with a self-assembled monolayer in OLEDs [J]. Synth Met, 2003, 138(2): 197-200.

[22] Vijila C, Pivrikas A, Chun H, et al. A study of charge transport in a novel electroluminescent poly(phenylene vinylene-co-fluorenylene vinylene) based p-conjugated polymer [J]. Org Electron, 2007, 8(1): 8-13.

[23] Martens H C F, Pasveer W F, Brom H B, et al. Crossover from space-charge-limited to recombination-limited transport in polymer light-emitting diodes [J]. Phys Rev B, 2001, 63(12): 125328-1-125328-7.

[24] Campbell A J, Bradley D D C, Lidzey D G. Space-charge limited conduction with traps in poly(phenylene vinylene) light emitting diodes [J]. J Appl Phys, 1997, 82(12): 6326-6342.

[25] Meyer H, Haarar D, Naarmann H et al. Trap distribution for charge carriers in poly(paraphenylene vinylene)(PPV) and its substitutes derivative DPOP-PPV [J]. Phys Rev B, 1995, 52(4): 2587-2598.

[26] Lupton J M, Samuel I D W, Beavington R, et al. Control of mobility in molecular organic semiconductors by dendrimer generation [J]. Phys Rev B, 2001, 63(15): 155206-1-155206-8.

(责任编辑 刘 钊)